Received: 24 January 2017 | Revised: 19 July 2017 | Accepted: 28 July 2017

DOI: 10.1002/hed.24941

ORIGINAL ARTICLE

WILEY

Genomic profiling of intestinal-type sinonasal adenocarcinoma reveals subgroups of patients with distinct clinical outcomes

Alejandro López-Hernández, MSc[1] | Jhudit Pérez-Escuredo, PhD[1] | Blanca Vivanco, MD, PhD[2] | Cristina García-Inclán, PhD[1] | Sira Potes-Ares, Bsc[1] | Virginia N. Cabal, BSc[1] | Cristina Riobello, MSc[1] | María Costales, MD, PhD[1] | Fernando López, MD, PhD[1] | José Luis Llorente, MD, PhD[1] | Mario A. Hermsen, PhD[1]

[1] Department of Otolaryngology, IUOPA, Hospital Universitario Central de Asturias, Oviedo, Asturias, Spain

[2] Department of Pathology, Hospital Universitario Central de Asturias, Oviedo, Spain

Correspondence
Mario A. Hermsen, Department of Otorrinolaringología, Instituto Universitario de Oncología del Principado de Asturias (IUOPA), Edificio FINBA, Lab ORL, Hospital Universitario Central de Asturias, Avenida de Roma s/n, 33011 Oviedo, Spain.
Email: mhermsen@hca.es

Funding information
This work was supported by Grants PI08-1599, PI11-929, PI13-646, and PI15-1629 from the Fondos de Investigación Sanitaria (FIS) and RD12/0036/0015 from the Red Temática de Investigación Cooperativa en Cáncer (RTICC), Spain; Plan Nacional de I+D+I 2008-2011 o el Plan Estatal de I+D+I 2013-2016, was co-financed by the FEDER Funding Program from the European Union.

Abstract

Background: Patients with intestinal-type sinonasal adenocarcinoma (ITAC) have an unfavorable prognosis and new therapeutic approaches are needed to improve clinical management.

Methods: Genetic analysis of 96 ITACs was performed by microarray comparative genomic hybridization and immunohistochemistry and correlated to previously obtained mutation, methylation, and protein expression data, and with pathological characteristics and clinical outcome.

Results: Seven copy number alterations (CNAs) were significantly associated with unfavorable clinical outcome: gains at 1q22-23, 3q28-29, 6p22, and 13q31-33, and losses at 4p15-16, 4q32-35, and 10q24. Unsupervised cluster analysis resulted in 5 subgroups of ITAC with significantly distinct genetic signatures and clinical outcomes, independently of disease stage or histological subtype.

Conclusion: These data may guide studies to identify driver genes and signaling pathways involved in ITAC. In addition, the subclassification of genetic subgroups of patients with distinct clinical behavior can aid therapeutic decision making and may ultimately lead to personalized therapy with targeted inhibitors.

KEYWORDS
copy number alteration, intestinal-type sinonasal adenocarcinoma (ITAC), mutation, protein expression, sinonasal adenocarcinoma

1 | INTRODUCTION

The sinonasal cavities harbor a wide variety of cancer types, approximately 25% of which are intestinal-type sinonasal adenocarcinoma (ITAC). The incidence is <1 case per 100 000 inhabitants per yea; however, among individuals with occupational exposure to wood and leather dust the risk of developing ITAC may be 500-900 times higher.[1–4] The ITAC is located almost exclusively in the ethmoid sinus and predominantly among men with a mean age of presentation of 60-65 years.[1,4] The World Health Organization classification of head and neck tumors distinguishes papillary, colonic, solid, and mucinous type, the latter 2 having a worse clinical behavior.[5] Distant and lymph node metastasis are exceptional.[6–8] Clinical management has improved owing to advances in diagnostic imaging techniques, less invasive

endoscopic surgical approaches, and precision radiotherapy, which achieves a better quality of life and may improve survival outcome.[4,9] Nevertheless, patients with ITAC still face an unfavorable prognosis, with a 5-year survival rate of 40%-60% and local recurrence often occurring within 2 years of follow-up being the main contributor to sinonasal cancer mortality.[3,5–11]

Partly due to its low incidence, relatively few studies have been dedicated to this tumor type. Nonetheless, our knowledge on the genetic aberrations in ITAC is increasing. Recent studies have shown a frequency of 40%–50% TP53 mutations and 50%-70% p53 overexpression.[12–16] Nuclear β-catenin expression was observed in approximately 30%–50%.[13,14,17,18] KRAS mutations were detected in 15% of ITAC, but none in B-type Raf (BRAF), epidermal growth factor receptor (EGFR), and adenomatous polyposis coli (APC).[13,17,19–24] Immunohistochemical studies on different receptor tyrosine kinases have shown 20%–30% EGFR, 8% erb-b2 receptor tyrosine kinase 2 (ERBB2), 64% cMET proto-oncogene, receptor tyrosine kinase (MET), and 0% anaplastic lymphoma receptor tyrosine kinase (ALK) overexpression, whereas fibroblast growth factor receptor 1 (FGFR1) gene copy number amplifications were absent.[22,23,25–28] The etiological factors wood and leather dust are not considered mutagenic, which is the reason why a role for inflammatory processes caused by a prolonged irritation by wood and leather particles has been suggested in ITAC tumorigenesis.[15,29,30] In accord with this hypothesis, cyclooxygenase-2 (COX-2) expression has been observed in up to 50% of ITAC and was correlated with wood dust but not tobacco exposure.[29,31] In addition, the dominant G>A missense mutations in TP53 and KRAS, found twice as frequent as tobacco-associated G>T, suggest a causal role for free radical species released by leukocytes in a chronic inflammatory environment.[12,15,32] Genomewide studies have been performed using comparative genomic hybridization (CGH) and microarray CGH.[33–36] In general, these studies have shown that ITAC harbor complex karyotypes with copy number alterations (CNAs) involving all chromosomes. Hotspot gains were found at 5p, 7, 8q, 12p, and 20q, and losses at 4q, 5q, 8p, 17p, and 18q.

Some of the above-described genetic abnormalities are also observed in histologically similar malignancies with much higher incidence, such as colorectal and lung adenocarcinoma. This is important because examples could be taken with regard to new therapies and clinical decision making; modern specific small molecule, or monoclonal antibody inhibitors in clinical use or in preclinical development for these more frequent tumor types may also work in ITAC if the same signaling pathways are affected.

The purpose of this study was to identify genetic profiles using a series of 96 clinically well-characterized ITACs, and to correlate the genetic results to pathological characteristics and clinical outcome. Previously obtained and published mutation data (TP53, EGFR, KRAS, and BRAF), protein expression data (p53, EGFR, and β-catenin), and gene methylation data, using part of the same series of tumors, were also used in the present analysis.[15,18,21,22] The results may increase our knowledge on the genetic pathways involved in ITAC tumorigenesis and identify molecular markers for prognosis and new therapies.

2 | MATERIALS AND METHODS

2.1 | Patients and tumor material

A total of 96 primary tumor samples were obtained from previously untreated patients seen between 1981 and 2010. Informed consent was obtained from all patients and the study was approved by the ethical committee of our institute. Ninety-three paraffin-embedded tissue samples were organized in a tissue microarray (TMA) and used for immunohistochemistry. From 60 cases, fresh frozen tissue material was obtained directly from the operating theater for DNA extraction using the Qiagen tissue extraction kit (Qiagen GmbH, Hilden, Germany). Two patients were women and 94 were men. The mean age was 66 years (range 48-92 years). Eighty-four had professional exposure to wood dust and 51 were tobacco smokers. Twenty-four tumors were disease stage I, 6 were stage II, 38 were stage III, 10 were stage IVa, and 18 were stage IVb.[37] No patient had metastases at the time of diagnosis. All cases in this study have been histologically evaluated by an experienced pathologist (B.V.) according to the World Health Organization histological classification,[5] 6 were papillary type or papillary tubular cylinder cell I (PTCC-I), 56 were colonic (PTCC-II), 9 were solid (PTCC-III), and 25 were mucinous type tumors. Cases showing more than 1 type were classified according to the worst histology. All patients underwent radical surgery with resection margins free of tumor. Sixty-one patients received complementary radiotherapy. Follow-up information was available with median of 61 months (range 1-264 months). A summary of all clinical data is given in Table 1.

2.2 | Microarray comparative genomic hybridization

Thirty-five cases were analyzed using a 30k oligonucleotide array printed on Codelink activated slides (Amersham Biosciences, Barcelona, Spain) and 25 using a 180k oligonucleotide array (SurePrint G3 Human CGH Microarray Kit 4 × 180K, Agilent Technologies, Palo Alto, CA), as described previously.[35,36,38] Images were acquired using a Microarray scanner G2505B (Agilent Technologies). Analysis and data extraction were quantified using feature extraction software version 9.1 (Agilent Technologies). Gains and losses were defined as deviations of 0.2 or more from log2

TABLE 1 Clinical data according to disease stage, histological subtype, and cluster

	Total	Stages I-III	Stage IV	*P* value	Papillary	Colonic	Solid	Mucinous	*P* value	Cluster I	Cluster II	Cluster III	Cluster IV	Cluster V	*P* value
Woodworker				.036					.020						.687
No	12/96 (13%)	5/68 (7%)	7/28 (25%)		0/6 (0%)	6/56 (11%)	4/9 (44%)	2/25 (8%)		2/24 (8%)	0/6 (0%)	0/15 (0%)	1/11 (9%)	0/4 (0%)	
Yes	84/96 (87%)	63/68 (93%)	21/28 (75%)		6/6 (100%)	50/56 (89%)	5/9 (56%)	23/25 (92%)		22/24 (92%)	6/6 (100%)	15/15 (100%)	1011 (91%)	4/4 (100%)	
Smoker				.455					.232						.687
No	45/96 (47%)	32/68 (47%)	13/28 (46%)		3/6 (50%)	22/56 (39%)	4/9 (44%)	16/25 (64%)		13/24 (54%)	4/6 (67%)	9/15 (60%)	5/11 (45%)	1/4 (25%)	
Yes	51/96 (53%)	36/68 (53%)	15/28 (54%)		3/6 (50%)	34/56 (61%)	5/9 (56%)	9/25 (36%)		11/24 (46%)	2/6 (33%)	6/15 (40%)	6/11 (55%)	3/4 (75%)	
Histology				.024					NA						.616
Pap	5/96 (8%)	6/68 (9%)	0/28 (0%)		...	...	...	...		4/24 (17%)	0/6 (0%)	0/15 (0%)	1/11 (9%)	0/4 (0%)	
Col	32/96 (53%)	44/68 (65%)	12/28 (43%)		...	...	...	...		12/24 (50%)	2/6 (33%)	10/15 (67%)	6/11 (55%)	2/4 (50%)	
Sol	5/96 (8%)	5/68 (7%)	4/28 (14%)		...	...	...	...		2/24 (8%)	0/6 (0%)	1/15 (7%)	1/11 (9%)	1/4 (25%)	
Muc	18/96 (28%)	13/68 (19%)	12/28 (43%)		...	...	...	...		6/24 (25%)	4/6 (67%)	4/15 (27%)	3/11 (27%)	1/4 (25%)	
Tumor stage				NA					.121						.361
I	24/96 (25%)	...	...		3/6 (50%)	15/56 (27%)	3/9 (33%)	3/25 (12%)		7/24 (29%)	2/6 (33%)	5/15 (33%)	3/11 (27%)	0/4 (0%)	
II	6/96 (7%)	...	...		0/6 (0%)	6/56 (11%)	0/9 (0%)	0/25 (0%)		1/24 (4%)	1/6 (17%)	0/15 (0%)	1/11 (9%)	0/4 (0%)	
III	38/96 (40%)	...	...		3/6 (50%)	23/56 (41%)	2/9 (22%)	10/25 (40%)		9/24 (38%)	2/6 (33%)	8/15 (53%)	3/11 (27%)	1/4 (25%)	
IVa	10/96 (10%)	...	...		0/6 (0%)	3/56 (5%)	1/9 (11%)	6/25 (24%)		3/24 (12%)	0/6 (0%)	2/15 (13%)	1/11 (9%)	0/4 (0%)	
IVb	18/96 (19%)	...	...		0/6 (0%)	9/56 (16%)	3/9 (33%)	6/25 (24%)		4/24 (17%)	1/6 (17%)	0/15 (0%)	3/11 (27%)	3/4 (75%)	
Intracranial				.001					.047						.001
No	83/96 (86%)	68/68 (100%)	15/68 (54%)		6/6 (100%)	52/56 (93%)	7/9 (78%)	18/25 (68%)		22/24 (92%)	6/6 (100%)	15/15 (100%)	7/11 (64%)	1/4 (25%)	
Yes	13/96 (14%)	0/68 (0%)	13/28 (46%)		0/6 (0%)	4/56 (7%)	2/9 (22%)	7/25 (32%)		2/24 (8%)	0/6 (0%)	0/15 (0%)	4/11 (36%)	3/4 (75%)	
Recurrence				.508					.027						.921
No	50/96 (52%)	37/68 (54%)	13/28 (46%)		5/6 (83%)	32/56 (57%)	1/9 (11%)	12/25 (48%)		13/24 (54%)	2/6 (33%)	8/15 (53%)	6/11 (55%)	2/4 (50%)	
Yes	46/96 (48%)	31/68 (46%)	15/68 (54%)		1/6 (17%)	24/56 (43%)	8/9 (89%)	13/25 (52%)		11/24 (46%)	4/6 (67%)	7/15 (47%)	5/11 (45%)	2/4 (50%)	
Metastasis				.023					.161						.846
No	82/96 (85%)	62/68 (91%)	20/28 (71%)		5/6 (83%)	51/56 (91%)	8/9 (89%)	18/25 (68%)		20/24 (83%)	5/6 (83%)	14/15 (93%)	9/11 (82%)	3/4 (75%)	
Yes	14/96 (15%)	6/68 (9%)	8/28 (29%)		1/6 (17%)	5/56 (9%)	1/9 (11%)	7/25 (32%)		4/24 (17%)	1/6 (17%)	1/15 (7%)	2/11 (18%)	1/4 (25%)	
Status				.001					.043						.476
Alive	33/96 (34%)	32/68 (47%)	1/28 (4%)		5/6 (83%)	22/56 (39%)	1/9 (11%)	5/25 (20%)		12/24 (50%)	2/6 (33%)	6/15 (40%)	3/11 (27%)	0/4 (0%)	
DOD	48/96 (50%)	25/68 (37%)	23/28 (82%)		1/6 (17%)	24/56 (43%)	7/9 (78%)	16/25 (64%)		9/24 (38%)	3/6 (50%)	6/15 (40%)	7/11 (64%)	4/4 (100%)	
DOOC	15/96 (16%)	11/68 (16%)	4/28 (14%)		0/6 (0%)	10/56 (18%)	1/9 (11%)	4/25 (16%)		3/24 (12%)	1/6 (17%)	3/15 (20%)	1/11 (9%)	0/4 (0%)	

Abbreviations: Col, colonic; DOD, died of disease; DOOC, died of other causes; Muc, mucinous; NA, not applicable; Pap, papillary; Sol, solid.
Stages I-III: disease stages I, II, and III; stage IV: disease stages IVa and IVb.

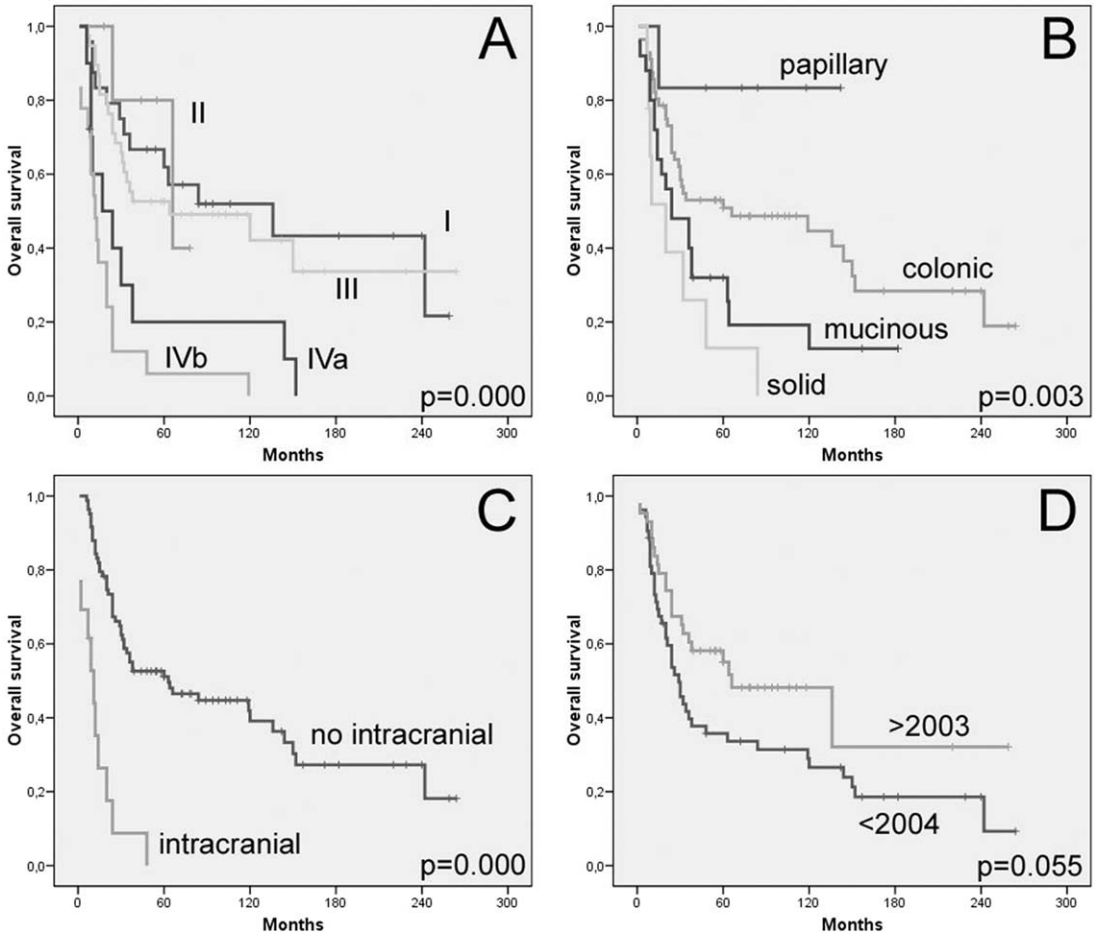

FIGURE 1 Kaplan-Meier overall survival analysis of 96 patients with intestinal-type adenocarcinoma according to disease stage A, to histological subtype B, intracranial invasion C, and year of treatment D

ratio = 0.0. Focal aberrations were defined as <3 Mbp size, with amplification showing log2 ratios of >2.0 and homozygous deletions log2 ratios of ≤3. Those focal aberrations overlapping with regions of normal copy number variation, as collected in the database of genomics variants, were excluded.

2.3 | Immunohistochemistry

A TMA consisting of 2 blocks of 2 × 2.5 cm, with tumor cores of 1-mm diameter separated by 1.5 mm was prepared from archival paraffin blocks. Each tumor was represented by 3 cores taken from different areas within an original paraffin block. A total of 96 ITAC tumors were represented in this TMA. Immunohistochemistry was performed with antibodies for intestinal mucosa marker CK20 (clone Ks20.8, DAKO, Glostrup, Denmark), proliferation marker Ki67 (clone Mib1, DAKO), and inflammatory pathway markers nuclear factor κ-light-chain-enhancer of activated B cells (NFκB; clone 20/NK-kBp65, BD Transduction Laboratories, Madrid, Spain) and COX2 (clone CX-294, DAKO) using an automatic staining workstation (Dako Autostainer; Dako Cytomation, Glostrup, Denmark) with the Envision system and diaminobenzidine chromogen as substrate. CK20 positivity was evaluated when either focal or diffuse cytoplasmic staining was observed. Ki67 staining was expressed as the percentage of nuclear-positive tumor cells. Nuclear staining of NFkB and cytoplasmic COX2 were scored as positive when >5% of tumor cells were positive.

2.4 | Statistical analysis

Possible correlations between genetic and clinical parameters were statistically analyzed by SPSS 15.0 software for Windows (SPSS, Chicago, IL), using the Pearson chi-square test, Fischer's exact test, and Student's *t* test. Multivariate Cox regression analysis was performed for factors possibly related to survival. The Kaplan-Meier analysis was performed for estimation of survival, comparing distributions of survival through the logarithmic range test (log-rank test). Values of $P < .05$ were considered significant. To analyze the presence of subsets of tumors with comparable patterns of chromosomal aberrations, and to analyze correlations between specific chromosomal aberrations, 2D hierarchical cluster analysis (statistical software R version 3.1.3) of the microarray CGH data was performed using 66 hotspot

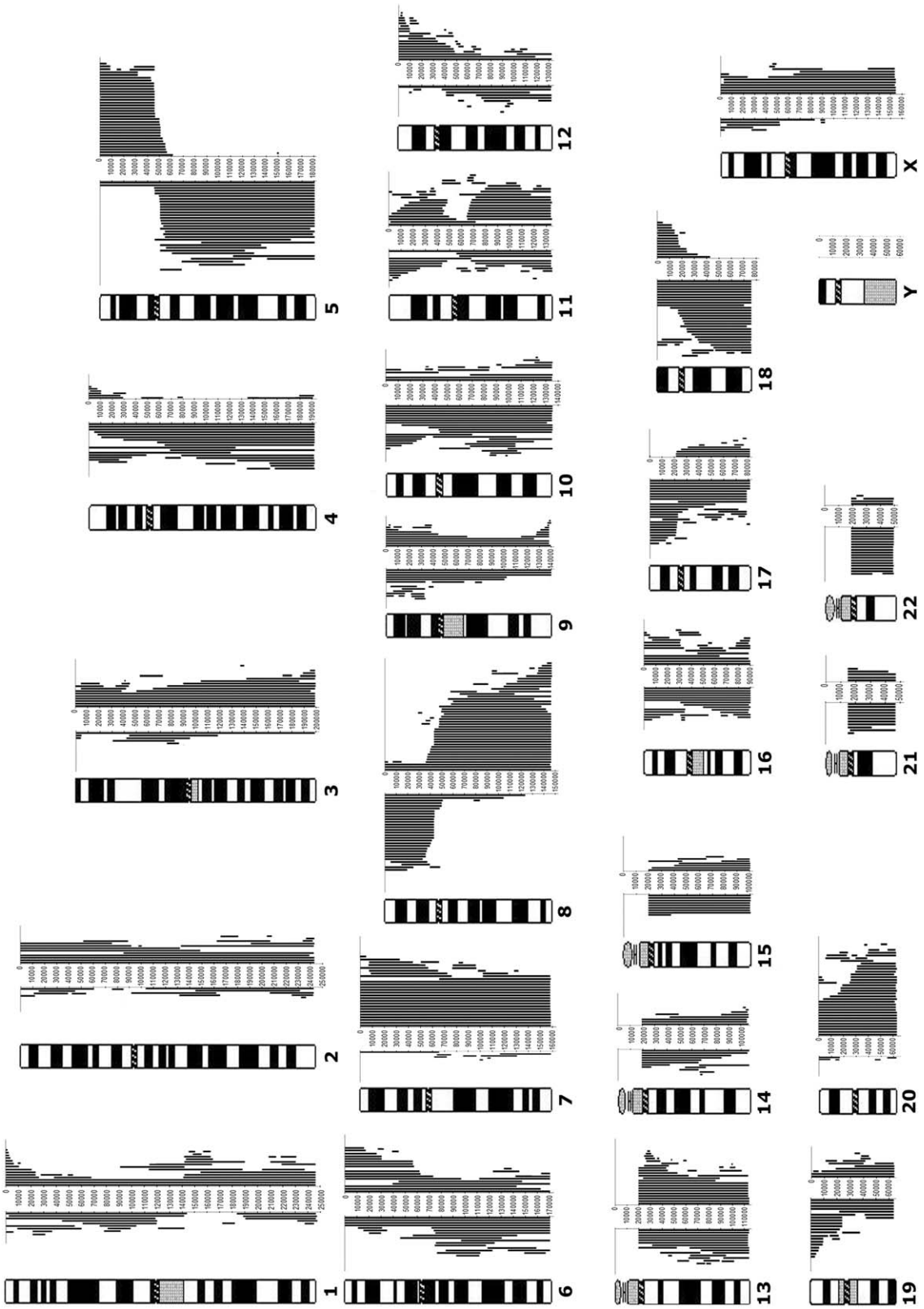

FIGURE 2 Overview of all copy number alterations as detected by microarray comparative genomic hybridization. To the right of the pictogram of each chromosome, a scale is placed expressing the number of megabase pairs (Mbps) counting from pter to qter. Copy number losses are presented as bars left to the Mbp scale and copy number gains to the right of the chromosome

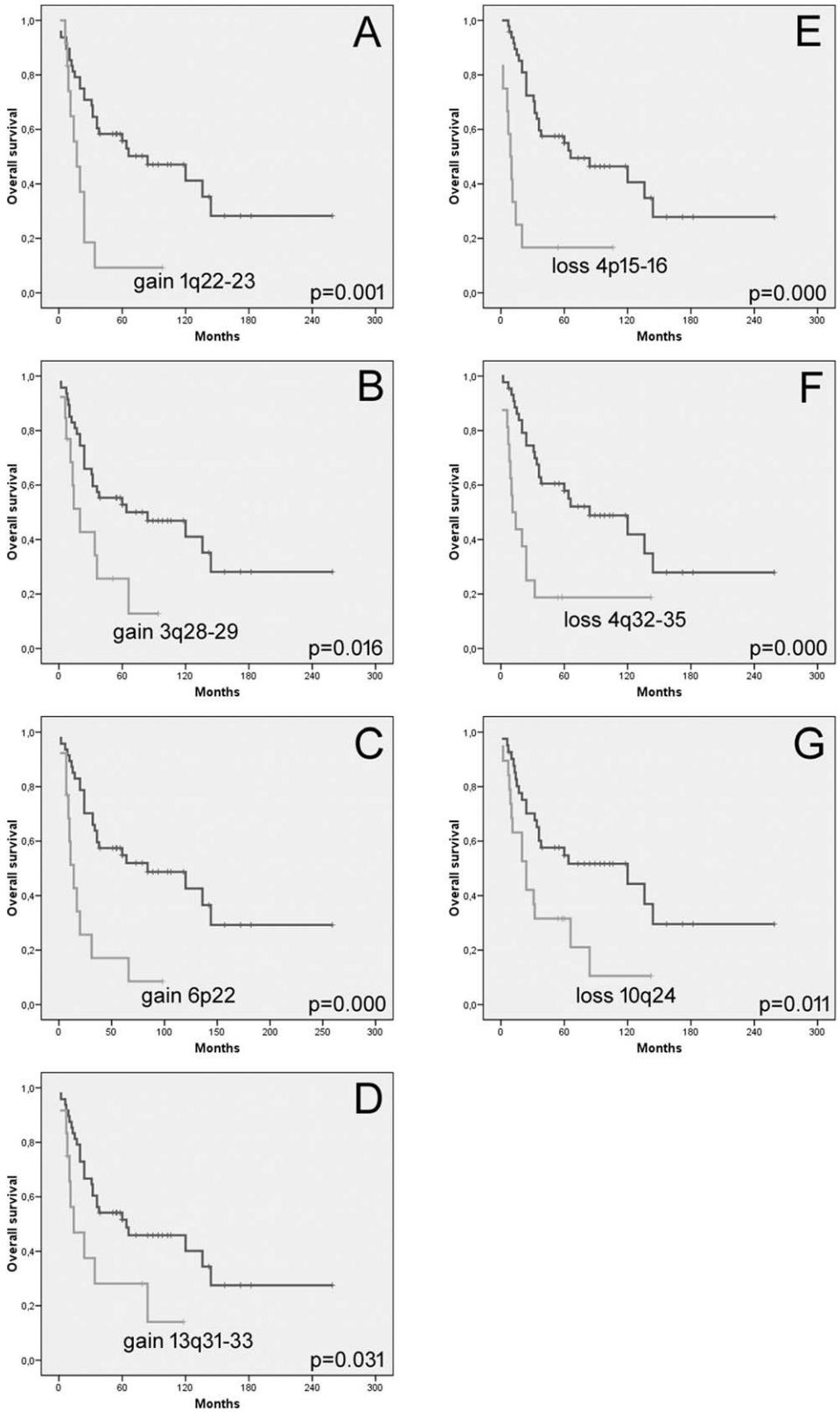

FIGURE 3 Kaplan-Meier overall survival analysis of 60 patients according to the presence of copy number gains at 1q22-23 A, 3q28-29 B, 6p22 C, and 13q31-33 D, and copy number losses at 4p15-16 E, 4q32-35 F, and 10q24 G

chromosomal areas showing gains and losses as input (Supporting Information Table S1). These areas were selected as showing copy number changes in >20% of the tumors. Only first-generation and second-generation clusters (ie, the first-level and second-level branches of the tree), were used for classification purposes.

TABLE 2 Genetic data according to disease stage, histological subtype and cluster

	Total	Stage I-III	Stage IV	*P* value	Papillary	Colonic	Solid	Mucinous	*P* value	Cluster I	Cluster II	Cluster III	Cluster IV	Cluster V	*P* value
Mutation KRAS	7/55 (13%)	6/40 (15%)	1/15 (7%)	.660	1/5 (20%)	6/31 (19%)	0 (0%)	0 (0%)	.237	2/24 (8%)	0/5 (0%)	2/13 (15%)	2/8 (25%)	1/4 (25%)	.590
Mutation TP53	14/41 (34%)	11/26 (42%)	6/15 (40%)	.999	1/3 (33%)	10/21 (48%)	3/5 (60%)	3/12 (25%)	.483	2/16 (13%)	0/5 (0%)	5/8 (63%)	6/8 (75%)	4/4 (100%)	.001
Expression p53	63/88 (72%)	47/63 (75%)	16/25 (64%)	.432	4/6 (67%)	40/52 (77%)	6/9 (67%)	13/21 (62%)	.599	11/21 (52%)	4/6 (67%)	11/14 (79%)	8/10 (80%)	4/4 (100%)	.223
Expression β-catenin	27/81 (33%)	21/58 (36%)	6/26 (26%)	.443	1/4 (25%)	20/51 (39%)	4/9 (44%)	2/17 (12%)	.173	5/18 (28%)	1/5 (20%)	5/11 (45%)	3/9 (33%)	1/4 (25%)	.828
Expression EGFR	18/87 (21%)	13/63 (21%)	5/24 (21%)	.999	1/6 (17%)	14/51 (27%)	2/9 (22%)	1/21 (5%)	.192	5/20 (25%)	0/5 (0%)	2/13 (15%)	2/8 (25%)	1/4 (25%)	.767
Expression NFκBp65	35/92 (38%)	23/66 (35%)	12/26 (46%)	.347	3/3 (50%)	23/54 43%)	5/9 (55%)	4/23 (17%)	.104	10/22 (45%)	1/6 (17%)	2/14 (14%)	6/10 (60%)	1/4 (25%)	.115
Expression COX2	34/87 (40%)	23/66 (35%)	11/24 (46%)	.467	2/6 (33%)	21/50 (42%)	6/9 (67%)	5/22 (23%)	.132	7/20 (35%)	2/6 (33%)	3/12 (25%)	2/10 (20%)	2/4 (50%)	.806
Expression CK20 (%)	66/86 (77)	52/62 (84)	14/24 (58)	.021	6/6 (100)	43/52 (83)	4/9 (44)	13/19 (68)	.031	12/18 (67)	5/6 (83)	9/13 (69)	8/10 (80)	2/2 (50	.762
Expression Ki67 %	19	20	17	.114	7	21	16	20	.597	17	11	38	20	15	.335
Methylation Methyl nr	1.22	1.03	1.71	.152	2.00	1.32	1.40	0.80	.310	1.67	0	0.82	1.00	2.75	.164
maCGH CNA nr	22.7	21.6	25.6	.425	10.0	25.6	23.8	20.6	.606	7.8	15.7	33.5	39.0	37.0	.001
maCGH Focal nr	6.5	6.9	5.6	.708	2.0	6.5	10.4	6.8	.554	2.0	4.8	11.7	11.4	3.3	.002
maCGH Amplif nr	2.3	2.2	2.5	.801	0	1.4	6.5	2.2	.212	1.3	2.0	2.0	3.6	0	.134

(Continues)

TABLE 2 (Continued)

	Total	Stage I-III	Stage IV	*P* value	Papillary	Colonic	Solid	Mucinous	*P* value	Cluster I	Cluster II	Cluster III	Cluster IV	Cluster V	*P* value
maCGH 1q+	12/60 (20%)	6/43 (14%)	6/17 (35%)	.081	0/5 (0%)	6/32 (19%)	2/5 (40%)	4/18 (22%)	.460	3/24 (13%)	0/6 (0%)	4/15 (27%)	2/11 (18%)	3/4 (75%)	.035
maCGH 3q+	13/60 (22%)	6/43 (14%)	7/17 (41%)	.035	0/5 (0%)	7/32 (22%)	2/5 (40%)	4/18 (22%)	.498	2/24 (8%)	3/6 (50%)	3/15 (20%)	2/11 (18%)	3/4 (75%)	.016
maCGH 4p-	12/60 (20%)	4/43 (9%)	8/17 (47%)	.002	0/5 (0%)	6/32 (19%)	1/5 (20%)	5/18 (28%)	.580	0/24 (0%)	0/6 (0%)	2/15 (13%)	7/11 (64%)	3/4 (75%)	.001
maCGH 4q-	16/60 (27%)	8/43 (19%)	8/17 (47%)	.049	1/5 (20%)	10/32 (31%)	1/5 (20%)	4/18 (22%)	.861	1/24 (4%)	0/6 (0%)	2/15 (13%)	9/11 (82%)	4/4 (100%)	.001
maCGH 6p+	13/60 (22%)	6/43 (14%)	7/17 (41%)	.035	0/5 (0%)	7/32 (22%)	2/5 (40%)	4/18 (22%)	.498	2/24 (8%)	1/6 (17%)	3/15 (20%)	5/11 (46%)	2/2 (50%)	.085
maCGH 10q-	19/60 (32%)	13/43 (30%)	6/17 (35%)	.763	1/5 (20%)	13/32 (41%)	3/5 (60%)	2/18 (11%)	.076	2/24 (8%)	1/6 (17%)	4/15 (27%)	9/11 (82%)	3/4 (75%)	.001
maCGH 13q+	12/60 (20%)	10/43 (23%)	4/17 (24%)	.293	1/5 (20%)	7/32 (22%)	3/5 (60%)	1/18 (6%)	.060	4/24 (17%)	0/6 (0%)	3/15 (20%)	1/11 (9%)	4/4 (100%)	.001

Abbreviations: Amplif nr, mean number of high level amplifications; CNA nr, mean number of copy number alterations; CK20, cytokeratin 20; COX2, cyclooxygenase-2; EGFR, epidermal growth factor receptor; Focal nr, mean number of focal aberrations; KRAS, V-Ki-ras2 Kirsten rat sarcoma viral oncogene homolog; Ki67, Antigen KI-67; maCGH, microarray comparative genomic hybridization; Methyl nr, mean number of methylated genes; NFκB, nuclear factor κ-light-chain-enhancer of activated B cells.

p53, cellular tumor antigen p53; Stage I-III: disease stages I, II, and III; stage IV: disease stages IVa and IVb; TP53, Tumor protein p53.

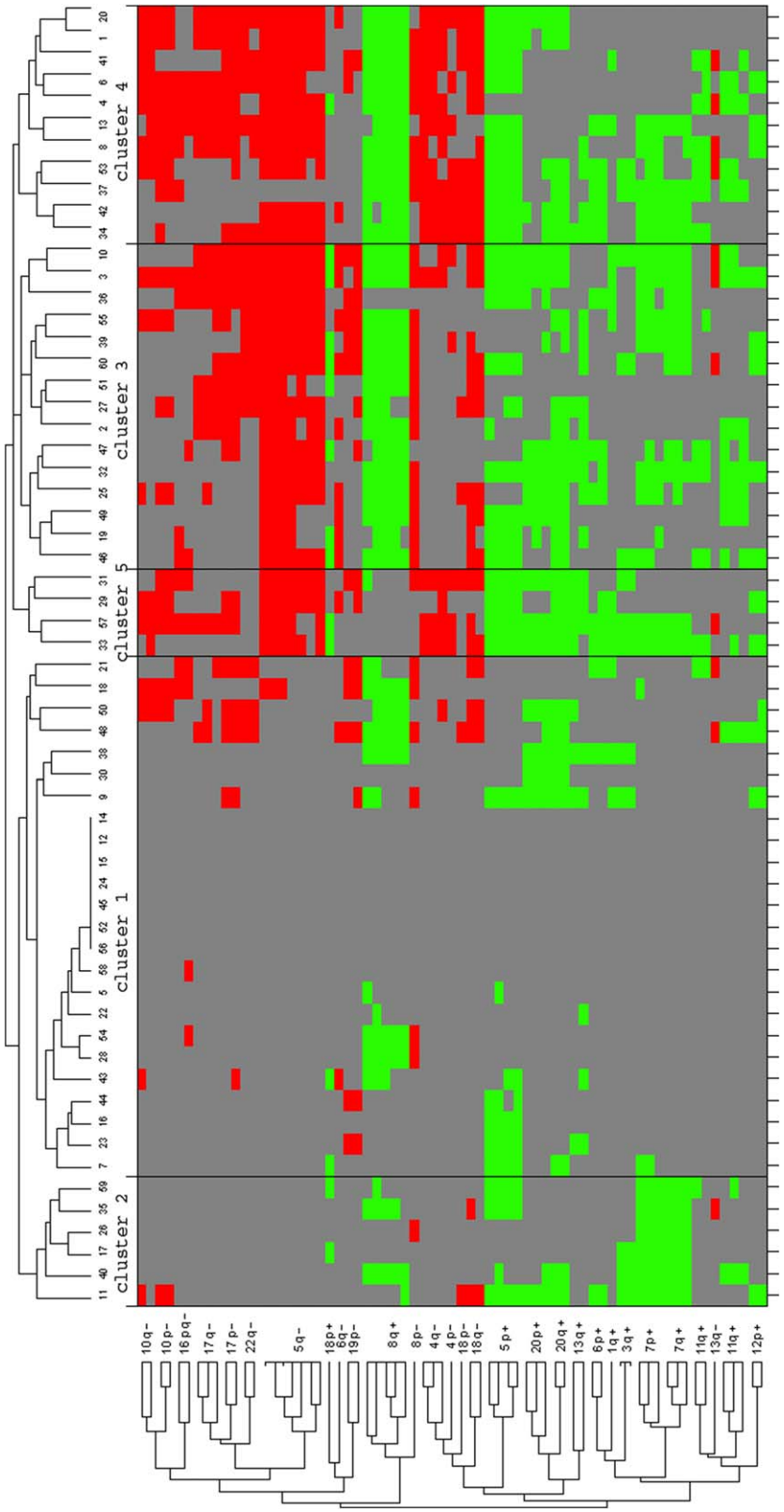

FIGURE 4 Heat map representation of the hierarchic cluster analysis of 60 intestinal-type adenocarcinomas based on 66 recurrent chromosomal gains and losses detected by microarray comparative genomic hybridization. Each row represents a specific chromosome region and every column represents a separate tumor. Bright gray cells indicate gain and dark gray cells indicate loss. Rows are ordered according to correlations between chromosomal changes, following the tree displayed on the left side. Tumors are grouped on the basis of similarities in chromosomal aberrations following the tree displayed on the top. Only first-generation and second-generation tumor clusters (the first-level and second-level branches of the tree) were used for classification purposes [Color figure can be viewed at wileyonlinelibrary.com]

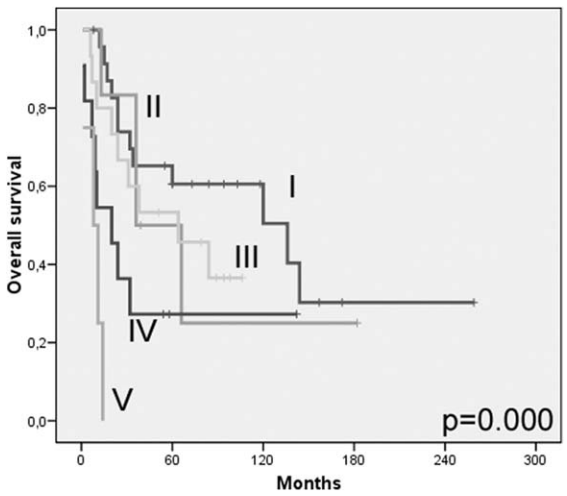

FIGURE 5 Kaplan-Meier overall survival analysis of 60 patients according to cluster

3 | RESULTS

3.1 | Follow-up

During the period of follow-up, 46 of 96 patients (48%) developed local recurrence and 14 patients (15%) developed distant metastasis, both with a median disease-free time of 9 months (range 1-96 months). At the time of writing, 33 of 96 patients (34%) remained disease-free (Table 1). The overall 5-year survival was 45% (36% for cases from 2003 and before and 55% for cases from 2004 and later), the main cause of death being local recurrence and intracranial invasion; however, 15 patients died during the postoperative period or due to intercurrent causes. Overall survival was significantly related to histological subtype (log-rank 14.291; $P = .003$), disease stage (log-rank 39.96658; $P = .001$), intracranial invasion (log-rank 32.913; $P = .001$) and the year of diagnosis (see Figure 1).

3.2 | Microarray comparative genomic hybridization

Microarray CGH revealed CNAs in 57 of the 60 cases. The major chromosomal regions showing gain or loss in >40% of cases were losses at 5q12-34, 8p21-22, 17p12-13, and 18q12-22 and gains at 5p12-ter, 7p14-21, 8q21-qter, and 20q11-qter (Figure 2, Supporting Information Table S1). Twenty-four regions harbored recurrent focal aberrations in 2 cases; focal gains at 14q11.2 and 19p13.3 and focal deletions at 4q13.2 were observed in 3 cases. In addition, recurrent high level amplifications were found at 8p11.23, 8q24.21 (2 separate ones), and 11q13.3 each occurring in 2 cases (Supporting Information Table S2). Univariate statistical analysis revealed 7 specific CNAs significantly associated with worse overall survival: gains at 1q22-23, 3q28-29, 6p22, and 13q31-33, and losses at 4p15-16, 4q32-35, and 10q24 (see Figure 3).

TABLE 3 Multivariate Cox regression survival analysis of disease stage, histological subtype and cluster

	Hazard ratio (95% CI)	Significance
Disease stage	1.62 (1.19–2.21)	$P = .002$
Histological subtype	1.25 (0.91–1.71)	$P = .162$
Cluster	1.52 (1.17–1.97)	$P = .002$

Abbreviation: CI, confidence interval.

Comparing disease stages I-III with stages IVa-IVb, we found no significant differences in the mean number of CNAs, focal aberrations, or amplifications. On the other hand, of the 7 prognostic CNAs, all except loss at 10q24 and gain at 13q31-33 were significantly more frequent in disease stage IVa-IVb tumors.

Papillar type ITACs harbored a mean number of 10 CNAs, much lower compared to colonic, solid, or mucinous types with mean CNAs of 26, 24, and 21, respectively. In addition, focal aberrations and amplifications occurred much less frequent in the papillary type (Table 2). The most recurrent (2/5 cases; 40%) alterations in papillary ITAC were gain of 5p and loss of 16p and 19p. Colonic, solid, and mucinous type tumors showed a similar profile of gains and losses, although the mucinous type seemed to carry them in a lower percentage of cases. With regard to the 7 prognostic CNAs, we found that the papillary type carried the lowest and the solid type ITAC the highest frequency.

A total of 66 hotspot regions showing recurrent gains and losses in at least 20% of cases were used for statistical analyzes. Hierarchic cluster analysis resulted in 5 groups of ITACs, based on the first-level and second-level branches of the tree (see Figure 4). Cluster 1 carried a significant lower mean number of CNAs than the other clusters, being 8 versus 33. Cluster 2 harbored a mean of 16 CNAs, also significantly lower than clusters 3, 4, and 5 with a mean CNA number of 34, 39, and 37 (Table 2). Apart from the number of alterations, the clusters also differed by their profile of CNAs (Supporting Information Table S1), particularly the 7 prognostic CNAs were observed in increasing frequency going from cluster 1 to cluster 5 (Table 2). Indeed Kaplan-Meier overall survival analysis showed a significantly better prognosis for cluster 1 and the worst prognosis for cluster 5, with clusters 2, 3, and 4 having intermediate survival curves (see Figure 5). Multivariate analysis revealed that cluster and disease stage remained their independent prognostic value, whereas histological subtype partly lost its correlation to overall survival (Table 3).

3.3 | Immunohistochemistry

Protein expression analysis by immunohistochemistry was performed on intestinal mucosa marker CK20, proliferation

marker Ki67, and inflammatory pathway markers COX2 and NFκBp65, complementing previously published stainings on p53, EGFR, and β-catenin. Strong membranous CK20 staining was observed in 66 of 86 analyzable cases (77%), with significantly less positive cases frequent with stages IVa-IVb. Solid type ITAC showed the lowest CK20 positivity, with only 4 of 9 cases (44%). Among the clusters, there were no great differences in CK20 expression. Proliferation marker Ki67 showed a mean of 19% positive tumor cells among all cases. Notably lower proliferation was seen in papillary cases (7%), and cluster III showed significantly more proliferation (38%). The NFκB and COX2 positivity was similar in disease stages I-III and stages IVa-IVb. The highest NFκB and COX2 expression occurred in solid type and the lowest positivity was seen in mucinous type ITAC. Clusters II and III demonstrated a lower percentage of cases with NFκB and COX2 positivity. Cluster IV showed frequent NFκB, but infrequent COX2 staining, and conversely cluster V showed infrequent NFκB but frequent COX2 expression (Table 2).

4 | DISCUSSION

The ITAC is a relatively rare tumor and, therefore, there are few genetic studies in the literature that analyzed a statistically relevant number of tumors. Even less studies have been able to correlate genetic findings with clinicopathological and follow-up data. In the present series of 96 tumors analyzed by microarray CGH and immunohistochemistry, we were able to recollect all relevant clinical, etiological, and pathological data and a mean follow-up time of 61 months, which is very high considering that the mean disease-free time is only 9 months. In terms of tumor stage, histological subtype, wood dust and tobacco exposure, and occurrence of recurrences and metastasis, our series is comparable with other published series.[1,5–8] The 45% 5-year overall survival was somewhat lower than previous series that reported 40%-60% survival or better.[3,5–11] This may be explained by the long period of recollection of patients (1981-2010). The 53 patients treated in the years 2004-2010 had a better 5-year overall survival than the 43 patients between 1981 and 2003 (55% vs 38%; log-rank 3.685; $P = .055$). In spite of this difference, our series does reflect the clinical characteristics known of ITAC, as indeed is demonstrated by prognostic value of disease stage, histological subtype, and intracranial invasion (see Figure 1). Therefore, we believe that the genetic alterations and clusters of cases with specific genetic profiles showing correlation to overall survival are valid.

The set of chromosomal regions showing recurrent gains and losses confirms previous studies on ITAC.[33–36] Some of these CNAs (gains at 7p, 8q, and 20q and losses at 8p and 17p) are found in the majority of all epithelial tumors. However, gains at 3q, 5p, 12p, and 18p and losses at 4q, 19p, and 22q observed in ITAC have not been reported in other adenocarcinomas, such as in colon and lung cancers. Conversely, frequent CNAs in lung and colon adenocarcinoma, for example, gain of 16p and losses of 9p and 15q were infrequent in ITAC.[39,40] Another peculiarity of ITAC is the very low occurrence of high-level amplifications (Supporting Information Table S2). Extending this comparison with other genetic data obtained in our previous studies,[15,18,21,22] we can add that frequent mutations in EGFR, KRAS, and BRAF, as found in lung cancer[40] as well as KRAS and BRAF in colon adenocarcinoma,[41,42] are absent or very infrequent in ITAC. These differences may reflect the different etiological factors involved (eg, inflammatory microenvironment in colon, tobacco in lung, and wood dust in sinonasal cavities).

It is difficult to speculate on specific genes on the basis of CNAs that span several megabase pairs. The 8 chromosomal regions with aberrations in >40% of cases all concerned large parts of chromosomal arms. However, high-level amplifications by definition englobe small areas carrying fewer genes. In the present series of ITAC, 4 overlapping amplifications were detected, each in 2 tumors (Supporting Information Table S2). At 11q13.3, the amplicon encompassed 7 genes, including the well-known oncogenes CCND1 and ORAOV1, but not, for example, EMS1 or FADD genes that are frequently coamplified with CCND1 and ORAOV1 in head and neck squamous cell carcinoma.[43,44] Chromosome 8p11 amplifications involving FGFR1 are found in many cancers, including oral, esophagus, breast, ovarian, and bladder cancer.[45] In the lungs, this amplification is frequent in squamous cell carcinoma but not in lung adenocarcinoma,[46] and the same was found in sinonasal cancer.[27] Our data on ITAC (also an adenocarcinoma) are in agreement with these findings, because the 8p11 amplification did not include FGFR1. Among the 5 genes that did localize within the amplicon, GPR124 is of interest as it functions as a coactivator of canonical β-catenin signaling,[47] a pathway active in 31% of ITAC.[18] At 8q24, we found 2 small amplifications. Curiously, 1 of them did not harbor any genes. The other contained 10 genes, 2 of which the cancer-related genes v-myc avian myelocytomatosis viral oncogene homolog (MYC) and *PFOU5F1B*. A recent article showed that PFOU5F1B, a pseudogene of OCT4, is transcriptionally active in gastric adenocarcinoma and confers an aggressive phenotype, enhanced by the additional overexpression of MYC.[48] Both ITAC cases carrying the amplification indeed showed adverse clinical characteristics. One was disease stage IVa mucinous type, the other a stage I solid type, both patients developed recurrent disease within the year and died of disease. A total of 27 recurrent focal aberrations were detected, occurring in 2 or 3 of the 60 tumors

analyzed (Supporting Information Table S2). Within these regions, we found few known cancer-related genes, examples are EGFR at 7p12 and STK11 at 19p13.3. Six focal aberrations harbored miRNAs that may merit further investigation.

Unsupervised cluster analysis performed on 66 defined CNAs resulted in 5 groups of tumors with distinct CNA profiles. Moreover, they significantly differed with regard to overall survival (see Figure 3). Multivariate analysis revealed that cluster and disease stage remained their independent prognostic value, whereas histological subtype partly lost its correlation to overall survival (Table 3). Subsequently, we set out to evaluate if ITACs grouped by stage, histological subtype, or by cluster would reveal unique clinicopathological, etiological, or genetic alterations, taking into account the CNAs and protein expression analyzes of this study (NFκB, COX2, CK20, and Ki67), as well as mutations (TP53, EGFR, KRAS, and BRAF), gene methylations (MS-MLPA), and protein expression (p53, β-catenin, and EGFR) previously published by our group.[15,18,21,22]

Disease stages I-III were not different from stages IVa-IVb with regard to mutations in KRAS or TP53, nor to expression of p53, β-catenin, EGFR, NFκB, COX2, or Ki67. CK20-positivity was significantly lower, whereas gene methylations and gains of 1q, 3q, and 6p and loss of 4p and 4q were more frequent in disease stages IVa-IVb (Table 2).

Solid type ITAC was less associated with wood dust than the other types, 56% versus 92%-100%. Both solid and mucinous types showed more intracranial invasion, with solid types developing more frequent recurrences and mucinous types more frequent metastases. Only papillary and colonic types showed KRAS mutations. This finding is in agreement with results in colorectal and lung cancers, in which KRAS was found to be frequent in early-stage tumors.[49,50] TP53 mutations were seen in all subtypes but least frequently in mucinous type (25% vs 33%-60%). Mucinous types also showed the lowest frequency of β-catenin, EGFR, NFκB, and COX2 staining (Table 2). CK20-positivity was lowest in the solid type. Gene methylation was more pronounced in the papillary type (mean number 2.0) and lowest in the mucinous type (mean number 0.8). A great difference in the number of CNAs was seen between papillary and the other subtypes. As reported previously,[34,35] papillary-type ITAC harbored only very few gains and losses; among them, the most frequent (40%) were gains at 5p and losses at 16p and 19p. Colonic, solid, and mucinous types of ITAC shared many CNAs, with the mucinous type generally having lower frequencies; however, gain of chromosome 7 was absent in the solid type and gain of 18p was especially frequent in the mucinous type. These data suggest that mucinous types of ITACs are genetically different from the other subtypes. This is in accord with immunohistochemistry data showing that mucinous types have less frequent p53-positivity and more frequent loss of membranous E-cadherin staining.[14,31] A similar observation has been reported for mucinous type adenocarcinomas of other organs, such as the colon, breasts, ovaries, and pancreas.[14,51,52]

The 5 clusters were not different with regard to wood or tobacco etiology. Although no relation was found between clusters and histological subtypes, cluster I had relatively more papillary type and cluster II more mucinous type tumors. Intracranial invasion was observed to be especially frequent in clusters IV and V, which is in agreement with these clusters having the worst prognosis. However, no clear differences were seen in the frequency of recurrence or metastasis. KRAS and TP53 mutations were mostly seen in clusters III, IV, and V, whereas p53-positivity increased from 50% to 100% going from cluster I to V. Nuclear β-catenin staining was observed in 20%-33% of all clusters and highest in cluster III (45%). The EGFR expression was present in 15%-25% but absent in cluster II. Gene methylation was most frequent in cluster V, but also cluster I showed a high number. No methylation was seen in cluster II. As the clusters were defined by the CNAs they harbored, great differences could be observed. First, clusters I and II had relatively few CNAs compared with the other clusters. In cluster I, alterations in $>20\%$ of cases were gains at 5p, 8q, 13q, and 20q and losses at 17p and 19p. Gain of whole chromosome 7 was absent in cluster I and occurred in 100% of cases in cluster II. Of notice in cluster V was the absence of a gain of 8q and a loss of 8p, which is 1 of the most frequent CNAs in ITAC and indeed in the majority of solid tumors. The 7 CNAs that showed prognostic value were observed in increasing frequency going from cluster I to V (Table 2), which is in accord with the increasing poor clinical outcomes of the clusters. Notably, in the whole group of tumors analyzed, these 7 CNAs were not among the most frequently detected alterations. All 7 consist of fairly large chromosomal areas, which is the reason why we cannot speculate on candidate driver genes within these regions.

Recent genetic profiling studies using integrated analysis of data from gene expression, exome sequencing, CNAs, methylation, microsatellite instability, and proteomics, have revealed distinct molecular subtypes. In lung adenocarcinoma, 3 expression profile clusters were identified, 1 marked by activation of EGFR and other tyrosine kinases and a relatively good prognosis, 1 by an inflammatory signature with mutations in NF1 and TP53, and 1 by a proliferative signature with KRAS activation and STK11 inactivation. When integrating these results with methylation, DNA ploidy, and CNA data, 6 molecular subtypes were defined.[40] In colorectal adenocarcinoma, Guinney et al[41] proposed 4 genetic subgroups: 1 with high gene methylation, microsatellite instability, and immune infiltration; 1 with high CNA, Wnt,

and Myc activation; 1 with high KRAS mutation and low CNA; and 1 with expression of mesenchymal factors. Another approach to molecular subtyping of colorectal adenocarcinoma is based on similarities to distinct cell types within the normal colon crypt: stem-cell like; inflammatory; transit amplifying; goblet-like; and enterocyte.[42] Importantly, these reported molecular subtypes are associated with different prognosis and with different response to treatments.

In conclusion, the CNA data presented in this study identified genetic subgroups with distinct clinical outcomes. Although further studies will be necessary to know which specific signaling pathways are involved in these subgroups, we identified 7 specific CNAs, gains at 1q22-23, 3q28-29, 6p22, and 13q31-33, and losses at 4p15-16, 4q32-35, and 10q24, significantly associated with the clusters and with poor outcome. It is important to realize that characterizing genetic subgroups of tumors is not a goal in itself but rather a means to guide therapeutic decision making. For that to become feasible in clinical practice, a reduced set of biomarkers for each of these molecular subtypes would need to be formulated and preclinical trials are needed to assess new targeted drugs performed. The results could be used to set up "personalized" therapeutic trials in a similar fashion, as is becoming the standard of care in lung cancer.

CONFLICT OF INTEREST

The authors declare no potential conflicts of interest.

AUTHOR CONTRIBUTIONS

Patient and clinical data collection: Costales, López, Llorente

Histopathological classification: Vivanco

DNA extraction: Potes-Ares, Cabal

Microarray CGH: López-Hernández, Pérez-Escuredo

Tissue preparation: Potes-Ares, Cabal, García-Inclán, Riobello

Immunohistochemistry: García-Inclán, Riobello

Data analysis: López-Hernández, Pérez-Escuredo, García-Inclán, Hermsen

Statistical analysis: López-Hernández, Pérez-Escuredo, Hermsen

Study design: Hermsen, Llorente, López-Hernández

Editing: Hermsen, Llorente, López, Costales, Vivanco, García-Inclán, Pérez-Escuredo, López-Hernández

Writing: López-Hernández, Hermsen, Pérez-Escuredo

ORCID

Fernando López, MD, PhD http://orcid.org/0000-0001-7019-9746

Mario A. Hermsen, PhD http://orcid.org/0000-0002-5959-6289

REFERENCES

[1] Lund VJ, Stammberger H, Nicolai P, et al. European position paper on endoscopic management of tumours of the nose, paranasal sinuses and skull base. *Rhinol Suppl.* 2010;22:1–143.

[2] IARC Working Group on the Evaluation of Carcinogenic Risks to Humans. Arsenic, metals, fibres, and dusts. *IARC Monogr Eval Carcinog Risks Hum.* 2012;100(Pt C):11–465.

[3] Youlden DR, Cramb SM, Peters S, et al. International comparisons of the incidence and mortality of sinonasal cancer. *Cancer Epidemiol.* 2013;37:770–779.

[4] Llorente JL, López F, Suárez C, Hermsen M. Sinonasal carcinoma: clinical, pathological and genetic advances for new therapeutic opportunities. *Nat Rev Clin Oncol.* 2014;11:460–472.

[5] Franchi A, Santucci M, Wening B. Adenocarcinoma. Barnes L, Evenson JW, Reichard P, Sidransky D, eds. *World Health Organization Classification of Tumours*. Pathology and genetics of head and neck tumours. Lyon, France: IARC; 2005: 20-23.

[6] Choussy O, Ferron C, Védrine PO, et al. Adenocarcinoma of ethmoid: a GETTEC retrospective multicenter study of 418 cases. *Laryngoscope.* 2008;118:437–443.

[7] Cantu G, Solero CL, Miceli R, et al. Anterior craniofacial resection for malignant paranasal tumors: a monoinstitutional experience of 366 cases. *Head Neck.* 2012;34:78–87.

[8] Bhayani MK, Yilmaz T, Sweeney A, et al. Sinonasal adenocarcinoma: a 16-year experience at a single institution. *Head Neck.* 2014;36:1490–1496.

[9] Nicolai P, Schreiber A, Bolzoni Villaret A, et al. Intestinal type adenocarcinoma of the ethmoid: outcomes of a treatment regimen based on endoscopic surgery with or without radiotherapy. *Head Neck.* 2016;38 Suppl 1:E996–E1003.

[10] Camp S, Van Gerven L, Poorten VV, et al. Long-term follow-up of 123 patients with adenocarcinoma of the sinonasal tract treated with endoscopic resection and postoperative radiation therapy. *Head Neck.* 2016;38(2):294–300.

[11] Vergez S, du Mayne MD, Coste A, et al. Multicenter study to assess endoscopic resection of 159 sinonasal adenocarcinomas. *Ann Surg Oncol.* 2014;21:1384–1390.

[12] Perrone F, Oggionni M, Birindelli S, et al. TP53, p14ARF, p16INK4a and H-ras gene molecular analysis in intestinal-type adenocarcinoma of the nasal cavity and paranasal sinuses. *Int J Cancer.* 2003;105:196–203.

[13] Yom SS, Rashid A, Rosenthal DI, et al. Genetic analysis of sinonasal adenocarcinoma phenotypes: distinct alterations of histogenetic significance. *Mod Pathol.* 2005;18(3):315–319.

[14] Franchi A, Palomba A, Fondi C, et al. Immunohistochemical investigation of tumorigenic pathways in sinonasal intestinal-type adenocarcinoma. A tissue microarray analysis of 62 cases. *Histopathology.* 2011;59:98–105.

[15] Pérez-Escuredo J, Martínez JG, Vivanco B, et al. Wood dust-related mutational profile of TP53 in intestinal-type sinonasal adenocarcinoma. *Hum Pathol.* 2012;43:1894–1901.

[16] Bossi P, Perrone F, Miceli R, et al. TP53 status as guide for the management of ethmoid sinus intestinal-type adenocarcinoma. *Oral Oncol.* 2013;49:413–419.

[17] Perez-Ordonez B, Huynh NN, Berean KW, Jordan RC. Expression of mismatch repair proteins, beta catenin, and E-cadherin in intestinal-type sinonasal adenocarcinoma. *J Clin Pathol.* 2004; 57:1080–1083.

[18] Díaz-Molina JP, Llorente JL, Vivanco B, et al. Wnt-pathway activation in intestinal-type sinonasal adenocarcinoma. *Rhinology.* 2011;49:593–599.

[19] Frattini M, Perrone F, Suardi S, et al. Phenotype-genotype correlation: challenge of intestinal-type adenocarcinoma of the nasal cavity and paranasal sinuses. *Head Neck.* 2006;28:909–915.

[20] Bornholdt J, Hansen J, Steiniche T, et al. K-ras mutations in sinonasal cancers in relation to wood dust exposure. *BMC Cancer.* 2008;8:53.

[21] López F, García Inclán C, Pérez-Escuredo J, et al. KRAS and BRAF mutations in sinonasal cancer. *Oral Oncol.* 2012;48:692–697.

[22] García-Inclán C, López F, Pérez-Escuredo J, et al. EGFR status and KRAS/BRAF mutations in intestinal-type sinonasal adenocarcinomas. *Cell Oncol (Dordr).* 2012;35:443–450.

[23] Projetti F, Durand K, Chaunavel A, et al. Epidermal growth factor receptor expression and KRAS and BRAF mutations: study of 39 sinonasal intestinal-type adenocarcinomas. *Hum Pathol.* 2013;44:2116–2125.

[24] Franchi A, Innocenti DR, Palomba A, et al. Low prevalence of K-RAS, EGFR and BRAF mutations in sinonasal adenocarcinomas. Implications for anti-EGFR treatments. *Pathol Oncol Res.* 2014;20:571–579.

[25] Franchi A, Fondi C, Paglierani M, Pepi M, Gallo O, Santucci M. Epidermal growth factor receptor expression and gene copy number in sinonasal intestinal type adenocarcinoma. *Oral Oncol.* 2009;45:835–838.

[26] Projetti F, Mesturoux L, Coulibaly B, et al. Study of MET protein levels and MET gene copy number in 72 sinonasal intestinal-type adenocarcinomas. *Head Neck.* 2015;37(11):1563–1568.

[27] Schröck A, Göke F, Wagner P, et al. Fibroblast growth factor receptor-1 as a potential therapeutic target in sinonasal cancer. *Head Neck.* 2014;36(9):1253–1257.

[28] Pacheco E, Llorente JL, López-Hernández A, et al. Absence of chromosomal translocations and protein expression of ALK in sinonasal adenocarcinomas. *Acta Otorrinolaringol Esp.* 2017;68: 9–14.

[29] Holmila R, Cyr D, Luce D, et al. COX-2 and p53 in human sinonasal cancer: COX-2 expression is associated with adenocarcinoma histology and wood-dust exposure. *Int J Cancer.* 2008; 122(9):2154–2159.

[30] Llorente JL, Pérez-Escuredo J, Alvarez-Marcos C, Suárez C, Hermsen M. Genetic and clinical aspects of wood dust related intestinal-type sinonasal adenocarcinoma: a review. *Eur Arch Otorhinolaryngol.* 2009;266(1):1–7.

[31] Vivanco Allende B, Perez-Escuredo J, Fuentes Martínez N, Fresno Forcelledo MF, Llorente Pendás JL, Hermsen M. Intestinal-type sinonasal adenocarcinomas. Immunohistochemical profile of 66 cases. *Acta Otorrinolaringol Esp.* 2013;64(2):115–123.

[32] Hold GL, El-Omar EM. Genetic aspects of inflammation and cancer. *Biochem J.* 2008;410:225–235.

[33] Ariza M, Llorente JL, Alvarez Marcos C, et al. Comparative genomic hybridization of primary sinonasal adenocarcinomas. *Cancer.* 2004;100:335–341.

[34] Korinth D, Pacyna-Gengelbach M, Deutschmann N, et al. Chromosomal imbalances in wood dust-related adenocarcinomas of the inner nose and their associations with pathological parameters. *J Pathol.* 2005;207:207–215.

[35] Hermsen MA, Llorente JL, Pérez-Escuredo J, et al. Genome-wide analysis of genetic changes in intestinal-type sinonasal adenocarcinoma. *Head Neck.* 2009;31:290–297.

[36] Pérez-Escuredo J, López-Hernández A, Costales M, et al. Recurrent DNA copy number alterations in intestinal-type sinonasal adenocarcinoma. *Rhinology.* 2016;54(3):278–286.

[37] Sobin LH, Gospodarowicz MK, Wittekind CH, eds. *International Union Against Cancer (UICC) TNM Classification of Malignant Tumors*, *7th edition*. Hoboken, NJ: Wiley-Blackwell; 2009.

[38] Pérez-Escuredo J, García Martínez J, García-Inclán C, et al. Establishment and genetic characterization of an immortal tumor cell line derived from intestinal-type sinonasal adenocarcinoma. *Cell Oncol (Dordr).* 2011;34(1):23–31.

[39] Nakao K, Mehta KR, Fridlyand J, et al. High-resolution analysis of DNA copy number alterations in colorectal cancer by array-based comparative genomic hybridization. *Carcinogenesis.* 2004; 25:1345–1357.

[40] The Cancer Genome Atlas Research Network. Comprehensive molecular profiling of lung adenocarcinoma. *Nature.* 2014;511 (7511):543–550.

[41] Guinney J, Dienstmann R, Wang X, et al. The consensus molecular subtypes of colorectal cancer. *Nat Med.* 2015;21(11):1350–1356.

[42] Sadanandam A, Lyssiotis CA, Homicsko K, et al. A colorectal cancer classification system that associates cellular phenotype and responses to therapy. *Nat Med.* 2013;19(5): 619–625.

[43] Gibcus JH, Menkema L, Mastik MF, et al. Amplicon mapping and expression profiling identify the Fas-associated death domain gene as a new driver in the 11q13.3 amplicon in laryngeal/pharyngeal cancer. *Clin Cancer Res.* 2007;13(21):6257–6266.

[44] Rodrigo JP, García-Carracedo D, García LA, et al. Distinctive clinicopathological associations of amplification of the cortactin gene at 11q13 in head and neck squamous cell carcinomas. *J Pathol.* 2009;217(4):516–523.

[45] Dienstmann R, Rodon J, Prat A, et al. Genomic aberrations in the FGFR pathway: opportunities for targeted therapies in solid tumors. *Ann Oncol.* 2014;25(3):552–563.

[46] Dutt A, Ramos AH, Hammerman PS, et al. Inhibitor-sensitive FGFR1 amplification in human non-small cell lung cancer. *PLoS One.* 2011;6(6):e20351.

[47] Posokhova E, Shukla A, Seaman S, et al. GPR124 functions as a WNT7-specific coactivator of canonical β-catenin signaling. *Cell Rep.* 2015;10(2):123–130.

[48] Hayashi H, Arao T, Togashi Y, et al. The OCT4 pseudogene POU5F1B is amplified and promotes an aggressive phenotype in gastric cancer. *Oncogene.* 2015;34(2):199–208.

[49] Kadota K, Sima CS, Arcila ME, et al. KRAS mutation is a significant prognostic factor in early-stage lung adenocarcinoma. *Am J Surg Pathol.* 2016;40(12):1579–1590.

[50] Watson R, Liu TC, Ruzinova MB. High frequency of KRAS mutation in early onset colorectal adenocarcinoma: implications for pathogenesis. *Hum Pathol.* 2016;56:163–170.

[51] Hanski C, Tiecke F, Hummel M, et al. Low frequency of p53 gene mutation and protein expression in mucinous colorectal carcinomas. *Cancer Lett.* 1996;103:163–170.

[52] Frumovitz M, Schmeler KM, Malpica A, Sood AK, Gershenson DM. Unmasking the complexities of mucinous ovarian carcinoma. *Gynecol Oncol.* 2010;117:491–496.

SUPPORTING INFORMATION

Additional Supporting Information may be found online in the supporting information tab for this article.

How to cite this article: López-Hernández A, Pérez-Escuredo J, Vivanco B, et al. Genomic profiling of intestinal-type sinonasal adenocarcinoma reveals subgroups of patients with distinct clinical outcomes. *Head & Neck*. 2017;00:000–000. https://doi.org/10.1002/hed.24941